A rotating ringdisk stripping technique used to study electroplating of Sn-Pb from methane sulfonic acid solutions

by J. Horkans
I. C. Hsu Chang
P. C. Andricacos

A rotating ring-disk stripping technique has been used to analyze Sn-Pb alloys plated from methane sulfonic acid solutions with and without a proprietary additive and to construct associated current-potential curves. The deposition of both pure Sn and pure Pb was polarized by the additive, but the polarization was much greater for Pb. For alloys plated without the additive, the potential dependence of the partial currents  $i_{Sn}$  and  $i_{Pb}$  was essentially the same as that of the pure metals. The alloy compositions were very different from the solution ratios Sn(II):Pb(II) and could be either tin-rich or lead-rich compared to the solution. In the presence of the additive, on the other hand, the alloy compositions approximated the solution

compositions of the metal ions; both Pb and Sn deposition were polarized in the alloy compared to deposition of the pure metals, but the extent of polarization caused by the codepositing metal was much greater for Sn. The electrodissolution of Sn-Pb alloys in HCl shows a complex oscillatory behavior, which is produced by the selective dissolution of Sn but which may also be sustained by the formation and redissolution of sparingly soluble surface films. The oscillatory behavior disappears at low dissolution current and low rotation rate, which favor a higher surface concentration of the dissolving metals. Composition determinations are essentially the same under conditions with and without oscillations.

Copyright 1993 by International Business Machines Corporation. Copying in printed form for private use is permitted without payment of royalty provided that (1) each reproduction is done without alteration and (2) the Journal reference and IBM copyright notice are included on the first page. The title and abstract, but no other portions, of this paper may be copied or distributed royalty free without further permission by computer-based and other information-service systems. Permission to republish any other portion of this paper must be obtained from the Editor.

### Introduction

Electroplated alloys, most notably Ni-Fe and Sn-Pb, have found wide applicability in the electronics industry in areas such as magnetic recording and interconnection technology (e.g. [1, 2]). Recent work [3–8] on the electrochemistry of the Ni-Fe plating system has demonstrated that alloy plating is a complicated process involving the simultaneous occurrence of several electrochemical reactions. It has also demonstrated, however, that adequate experimental, theoretical, and computational tools are available to researchers to develop an understanding of the interrelationship between convective diffusion, electrode potential, and the surface and bulk concentrations of the various species that compose a plating solution. Although electroplated Sn-Pb is another alloy important to the electronics industry, similar work on the Sn-Pb system is lacking. It is the intention of this paper to present an experimental method by which such understanding can be obtained and to provide an initial description of Sn-Pb plating from a recently developed type of solution, namely one in which the supporting electrolyte is methane sulfonic acid (designated as MSA).

Work done in our laboratory [9-11] has shown that rotating ring-disk electrodes (RRDEs) are valuable tools for the study of Sn-Pb and other alloy plating systems. Following the deposition of the alloy on the disk electrode under the desired conditions of solution composition, current density, temperature, and agitation, the electrode is transferred to an appropriately engineered stripping medium where the deposited alloy is anodically dissolved under controlled conditions. The ring electrode is used as a collector to detect the component of the dissolving alloy that can change oxidation state (Sn, in the case of Sn-Pb). The total oxidation charge passed at the ring electrode (from which the Sn content of the plated alloy is determinable) and the total stripping charge passed at the disk electrode (which is the total of the Pb and Sn) yield the composition of the plated alloy, and a comparison of the disk dissolution charge with the plating charge yields the current efficiency of the process.

The Sn(II) detection, which requires sufficiently fast oxidation kinetics at the ring, dictates the use of an acidic chloride stripping medium and a Au ring electrode. [See, e.g., Mandler and Bard et al. [12] for a discussion of the Sn(II)/Sn(IV) kinetics.] We have found previously that the best results are obtained using a solution of 2 N HCl. With the Au ring potentiostatted at a potential in the range 0.30 to 0.65 V vs. SCE (saturated calumel electrode), the Sn(II)  $\rightarrow$  Sn(IV) +  $2e^-$  ring reaction occurs under total mass transport control, and the collection efficiency of the RRDE, calculated from the geometry of the ring-disk electrode, can be used in the calculation of the deposit composition. Compositions of alloys plated

from fluoborate solutions and determined by RRDE analysis were found to agree well with compositions determined by an independent technique, such as alloy dissolution in HNO<sub>3</sub> and determination of metal ion concentrations by inductively coupled plasma atomic absorption [10].

### **Experimental methods**

The methane-sulfonic-acid-based Sn-Pb plating system was purchased as its components from LeaRonal, Freeport, NY. The Sn(II)- and Pb(II)-containing solutions were prepared from the LeaRonal concentrates. These have known metal ion concentrations, which have been verified by polarography. The tin concentrate is thought to contain an antioxidant. The methane sulfonic acid was purchased separately as an analytical-grade reagent.

The alloy was plated on the disk of a Pine Instruments DT21 RRDE controlled by a Pine Instruments analytical rotator. The electrode had a disk area of 0.20 cm<sup>2</sup>, a ring area of  $0.16 \text{ cm}^2$ , and a collection efficiency N of 0.39. The plating was accomplished with a Pine Instruments RDE4 potentiostat in the galvanostatic mode, recording the potential. The charge was monitored with an EG&G Model 179 coulometer. A jacketed cell was used, and the temperature was controlled at 25°C. Solutions were deoxygenated thoroughly with bubbling N<sub>2</sub>; the presence of O<sub>2</sub>, however, had little effect on the measurements. A Pt anode was in a compartment separated from the working electrode by a glass frit. The reference electrode compartment was joined to the cell by a Luggin capillary positioned below the RRDE. The reference electrode was Hg/Hg,SO<sub>4</sub>/(sat.)K,SO<sub>4</sub>, referred to as a mercury sulfate electrode (MSE); it has a potential of 0.64 V vs. NHE (normal hydrogen electrode) or 0.40 V vs. SCE. A double junction was used to prevent the formation of insoluble PbSO<sub>4</sub>; the internal solution was 0.1 N MSA.

The plating potentials were corrected for the uncompensated resistance  $R_{\rm u}$  of the electrolyte between the reference and working electrodes. The  $R_{\rm u}$  value was measured in a solution of 0.2 M Pb(II) in 1 N MSA using a Stonehart BC1200 potentiostat and was found to be 3.85  $\Omega.$ 

The plating solutions had a total acid concentration of 1 N MSA. The compositions of the solutions used are shown in **Table 1**. The additive was measured in volume percent of the concentrate added.

It is undesirable to plate the Sn-Pb directly on the Pt disk, because in highly acidic solution  $H_2$  evolution is more favorable on Pt, both kinetically and thermodynamically, than the alloy deposition. An underlayer with lower catalytic activity for  $H_2$  evolution was thus used between the Sn-Pb alloy and the Pt disk. Copper underlayers were investigated initially and found not to interfere with the stripping analyses. The ultimate choice

**Table 1** Compositions of plating solutions (in 1 N MSA). Plating was carried out at 400 rpm.

PB(II) (molar)	Sn(II) (molar)	Additive (vol. %)
0.2	_	
0.2	_	10
	0.2	
_	0.2	10
0.2	0.1	10
0.2	0.2	_
0.2	0.2	10
0.2	0.3	10
0.2	0.4	_
0.2	0.4	10
0.2	0.5	_
0.2	0.4	0.5
0.2	0.4	1
0.2	0.4	5

of the underlayer, however, was Ni. Neither Ni nor Cu interfered with the stripping analysis, and the elimination of Cu removed any possibility of the formation of Cu-Sn intermetallics.

The cleaning procedure was critical to achieving reliable and reproducible measurements; unless the Au ring is clean and active, it does not detect Sn(II) quantitatively. The RRDE was first polished briefly using a wheel with 0.05  $\mu$ m alumina on a polishing cloth. It was then cleaned in 10% HNO<sub>3</sub>. The Ni was plated on the Pt disk at 10 mA/cm² to a thickness of 0.6 C/cm² (about 200 nm) at a rotation rate of 400 rpm. Then the Sn, Pb, or alloy was plated to 5 C/cm² (about 7.0  $\mu$ m of Sn or 4.5  $\mu$ m of Pb) at 400 rpm.

The electrode was immediately removed to a stripping solution. The pure metals were stripped potentiodynamically in 1 N MSA. The potential was swept at 2 mV/s toward more positive potentials starting at -1.0 V vs. MSE, rotating the electrode at 2500 rpm. The stripping charge, which had a clear end point, was measured with an EG&G PAR Model 379 coulometer. The stripping peaks from Sn and Pb were located at about -0.8 V, with the Ni not stripping until a potential of about -0.43 V. Alloy compositions could only be determined in HCl stripping solutions, which permitted determination of the Sn(II) at the ring. Alloys were stripped galvanostatically at either 10 or 20 mA/cm<sup>2</sup> in 2 N HCl; the rotation rate was 2500 rpm. The ring was maintained at a potential of +0.1 V. The ring charge was measured with a second Model 379 coulometer. It was verified that Sn(II) is quantitatively detected at the ring under these conditions. Fresh HCl stripping solution was used for each measurement. This stripping technique has been previously verified by comparison with inductively coupled plasma analyses of Sn-Pb alloys [10].

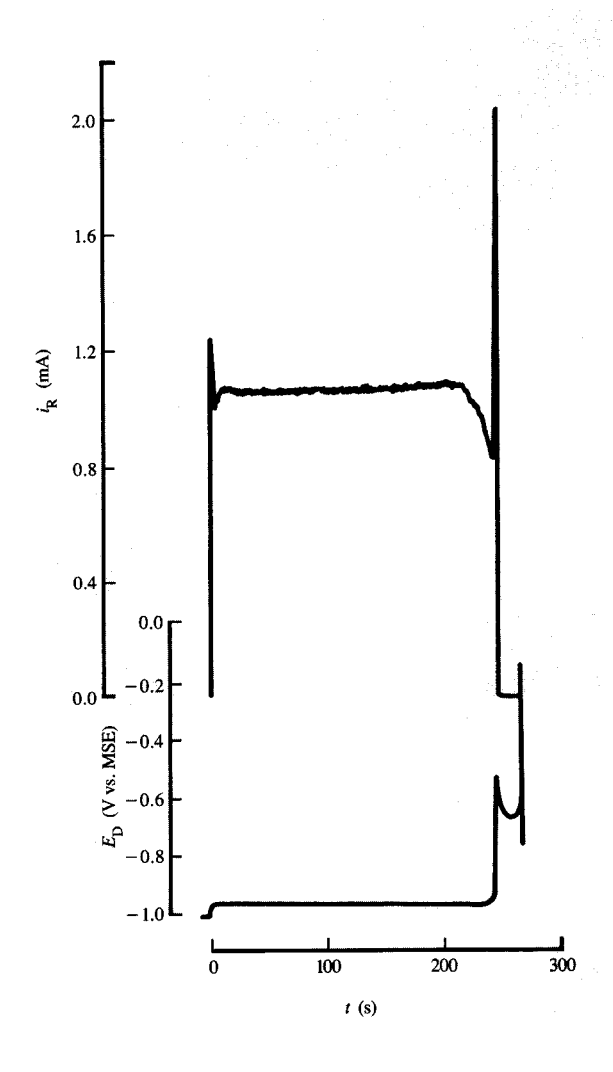


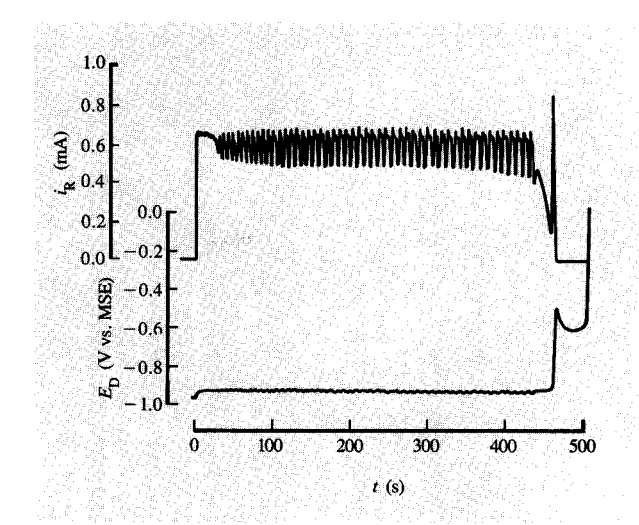
#### Figure 1

Stripping of a Sn–Pb alloy film plated to 1.0 C on a disk having an area of  $0.20~\text{cm}^2$ . The plating was carried out at 30 mA/cm² from a solution containing 0.2 M Pb(II), 0.3 M Sn(II), 1 N MSA, and 10 vol. % additive. The stripping current was 4 mA; the ring potential was +0.1~V vs. MSE; the rotation rate was 2500 rpm. The  $\chi_{Sn}$  of the alloy was 70.4 at. %.

# Results and discussion

# • Stripping behavior

Galvanostatic stripping analysis passes a constant oxidizing current at the disk: The reaction at the disk is  $M \to M(II) + 2e^-$ , where M is either Sn or Pb. A constant potential at the Au ring oxidizes the stannous tin: Sn(II)  $\to$  Sn(IV) +  $2e^-$ . The disk potential and the ring current are monitored as a function of time. An illustrative stripping curve is shown in **Figure 1**. When the



Stripping of a Sn-Pb alloy film plated under the conditions of Figure 1. The stripping current was 2 mA; the other stripping conditions were the same as in Figure 1.

current is applied and alloy dissolution commences, the disk potential becomes slightly more positive. Simultaneously, the Sn(II) oxidation current flows at the ring. When the Sn-Pb dissolution is complete and Ni dissolution commences, the disk potential rises abruptly to the value of Ni dissolution, and the ring current drops to zero. Dissolution of Ni is followed by Cl, evolution, evidenced by a large increase in the disk potential and by a reducing current at the ring. The flow of current from Cl, reduction on the ring does not interfere with the Sn(II) determination, however; it is in the opposite direction from the Sn(II) oxidation current and is not recorded by the coulometer, which registers only the anodic charge. The product of the disk current  $i_D$  and the time to the potential rise is the total metal charge:  $Q_{\rm D}$  =  $Q_{\rm Sn}$  +  $Q_{\rm Pb}$ . The tin charge can be determined from the total ring charge,  $Q_{\rm Sn}$  =  $Q_{\rm R}/N$ , where N, the collection efficiency of the ring-disk electrode, is a function of the radius of the disk and the inner and outer radii of the ring [13]. At any point on the curve, the ring current  $i_R$  is related to the Sn(II) portion of the instantaneous flux  $i_{Sn}$  of dissolving metal by  $i_{Sn} = i_R/N$ .

The Sn-Pb alloy film of Figure 1 was plated at 30 mA/cm<sup>2</sup> from an additive-containing solution of 0.2 M Pb(II), 0.3 M Sn(II), 1 N MSA, and 10 vol. % of additive. The stripping was done at 4 mA (20 mA/cm<sup>2</sup>). The disk and ring charges during stripping yielded an average composition of 70.4 at. % Sn. In every alloy plated, the layer stripped immediately before the Ni

appeared to be pure Sn. (At a stripping current of 4 mA, pure Sn would produce a ring current of  $N \times i_D = 1.6$  mA. The apparent ring current of >1.6 mA in Figure 1 is an artifact of overshoot of the Y-t recorder. This final Sn peak at the interface generally has a value very near  $N \times i_{\rm p}$ .) The apparent thickness of this Sn layer varies with the composition of the alloy plated and ranges from that of the very thin layer of Figure 1 to perhaps a hundred nanometers. The layer stripped just before this Sn interfacial layer is always Sn-poor compared to the rest of the film. The segregation of the Sn at the Ni interface may be an artifact of either the plating or the stripping. A separate analytical technique, such as Auger profiling, would be required to confirm the presence of the interfacial Sn layer. In general, anodic stripping gives reliable information about the average composition of plated materials. Radial composition variations will not be detectable. Variations with thickness may not be reflected in the dissolution profile; in fact, the electrodissolution may cause segregation through selective processes.

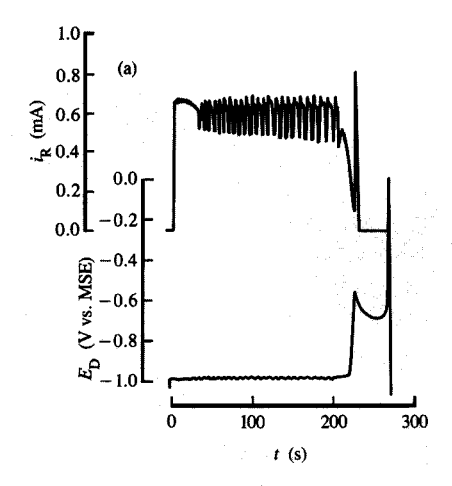
The stripping behavior of Sn-Pb varies with the conditions of electrodissolution. When the film of Figure 1 is dissolved at a lower current, 2 mA, the stripping curves of Figure 2 are obtained. Superimposed on an average ring current of 0.56 mA are large oscillations. The ring-current oscillations accompany oscillations of the disk potential of only a few millivolts, implying that gross changes in the disk chemistry are not occurring. The integrated ring charges are the same for stripping currents of 4 mA, when no oscillations are observed, and 2 mA, when they are. A lower stripping current generally results in a slightly lower disk charge. The different stripping conditions, however, give essentially the same values of alloy composition.

The effect of film thickness on the oscillations is shown in **Figure 3**. Films 0.5, 0.25, and 0.12 times the thickness of that of Figure 2 were stripped under the same conditions. The initial portion (about 30 s) and final portion (about 20 s) of the stripping behavior are invariant with film thickness; the duration of the intermediate oscillations is decreased in thinner deposits. The initial portion of the curve may reflect the time necessary to develop the conditions causing the oscillations and may not reflect a real difference between surface and bulk composition. The thickness-independence of the final portion may be evidence that the thin Sn layer at the Ni interface is present in the as-plated film and is not produced by the stripping.

Lowering the rotation rate of the RRDE during stripping reduces the extent of oscillation. Figure 4 shows the stripping of the same deposit at the same 2-mA current as in Figure 2, but at 1600 rpm rather than the usual 2500 rpm. Only one small spike is observed in an otherwise constant ring current, just before the Sn-poor layer near the Sn/Ni interface. At an even lower rotation rate, 900 rpm, the ring

current is constant except for the Sn-poor layer near the substrate and the thin interfacial layer of pure Sn.

Many variations of the oscillatory stripping behavior were observed; examples are given in **Figures 5** and **6**. An alloy plated at 30 mA/cm² from an additive-free solution containing 0.2 M Pb(II) and 0.4 M Sn(II) dissolves at 2 mA, as shown in Figure 5. The tin content  $\chi_{\rm Sn}$  of the film is 54.5 at. %. The ring current has one large oscillation around the average value of 0.45 mA, then ends with the Sn-rich interfacial layer. Plating at 80 mA/cm² from the same solution yields an alloy with  $\chi_{\rm Sn}=70.7$  at. % and the stripping behavior of Figure 6. This composition is nearly the same as that giving the behavior of Figure 2 under



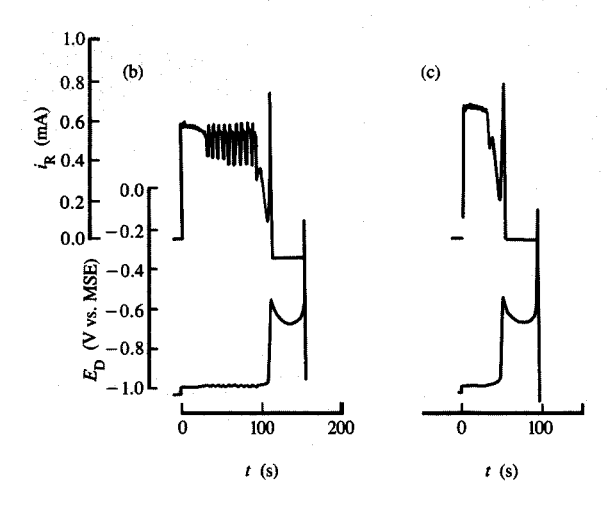


# Figure 3

Stripping of Sn-Pb alloy films plated under the conditions of Figure 1, but to total charges of (a) 0.5 C, (b) 0.25 C, and (c) 0.12 C. The stripping current was 2 mA, as for Figure 2.

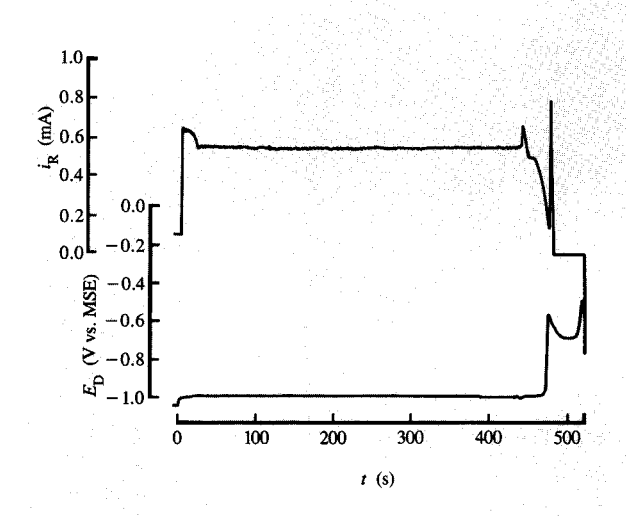


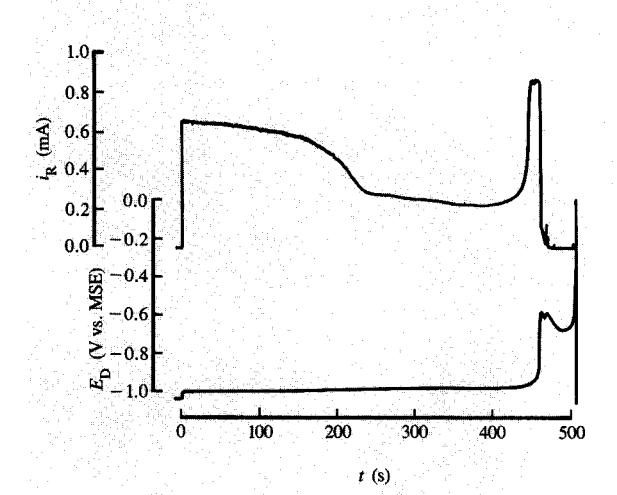
## Figure 4

Stripping of a Sn-Pb alloy film plated under the conditions of Figure 1, but at a rotation rate of 1600 rpm rather than 2500 rpm.

identical stripping conditions. Other alloy films with  $\chi_{\rm Sn}=62.9$  at. % and  $\chi_{\rm Sn}=55.1$  at. % showed one or several oscillations during the first ~50 s of stripping, followed by a constant ring current until the film was nearly removed, and then two more current oscillations just before the Sn-poor layer near the substrate. All of the stripping curves were extremely reproducible in the number of oscillations, their frequency, and their positions.

Oscillations during anodic dissolution have been observed in a variety of systems. A review of the literature to about 1971 was published by Wojtowicz [14]. The most extensively studied system is the dissolution of Cu in HCl [15–19], but oscillatory behavior can appear in many systems in which the formation of passivating surface films occurs [20–24]. The behavior of an alloy is more complicated, however, because of the additional possibility of preferential dissolution of one of the components. Preferential dissolution is strongly suggested by the stripping curves, which always show the highest ring current in the initial stages of dissolution. The variety of the observed oscillations, however, indicates that film formation may play a role in addition to the preferential dissolution.

The occurrence of oscillations during stripping is related to the alloy composition and structure. Under conditions favoring oscillations (2-mA stripping current and 2500-rpm rotation rate), no oscillations have been observed in alloys with Sn contents above ~75 at. % or below ~55 at. %. Alloy films of the same composition may not show the same behavior, as exemplified in Figures 2 and 6. In



Stripping of a Sn-Pb alloy film under the conditions of Figure 2; the Sn content of the film was 54.5 at. %. It was deposited at 30 mA/cm<sup>2</sup> from a solution consisting of 0.2 M Pb(II) and 0.4 M Sn(II) in 1 N MSA.

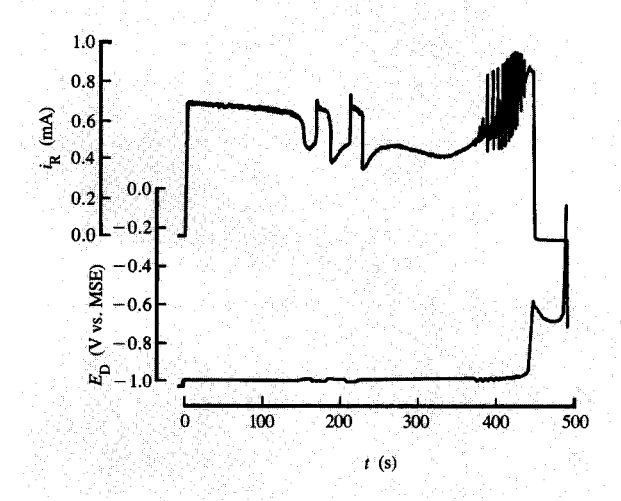


# Figure 6

Stripping of a Sn-Pb alloy film under the conditions of Figure 2; the Sn content of the film was 70.7 at. %. It was deposited at 80 mA/cm<sup>2</sup> from the solution of Figure 5.

general, fewer oscillations are observed when stripping deposits from additive-free solutions, which tend to be rougher than those from solutions with additives. Thus, the oscillations are probably related to structure as well as to composition. It may be difficult to maintain coherent surface precipitates on rough structures. Additionally, the preferential dissolution of the Sn may create rough or porous surface layers that influence the oscillatory behavior.

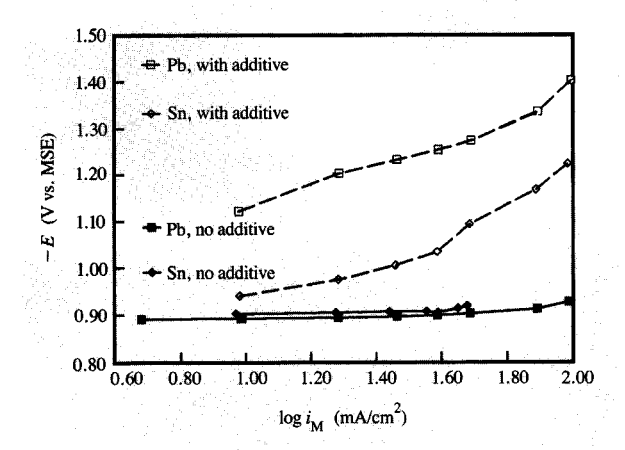
Deposits with low Sn levels never reach a stripping end point, presumably because of the formation of sparingly soluble surface films. Of the likely species during anodic dissolution of Sn-Pb alloys in HCl, the least soluble is  $PbCl_2$ , which has a solubility constant of  $\sim 10^{-4.7}$  [25]. Higher complexes of Pb(II) can form, keeping the lead in solution at high  $Cl^-$  concentrations [26]. The surface ratio of the Pb(II) to the  $Cl^-$  determines whether a film will precipitate. The conditions that reduce oscillations (lower rotation rate and higher dissolution current) are those that cause the M(II): $Cl^-$  ratio at the electrode surface to be relatively high.

The electrodissolution of Sn-Pb is characterized by the initial preferential dissolution of Sn. When the surface concentration of Pb is thus enriched, a period of enhanced Pb(II) flux ensues, and favorable conditions for PbCl, precipitation occur. With high rotation rates and low disk currents, this film is not stable; these are the conditions under which oscillations are observed. The complete description of this behavior is not yet possible. The original intent of this investigation, however, was not to study the stripping behavior but rather to use the stripping procedure to understand Sn-Pb plating. Thus, a full attempt to explain the oscillations during the electrodissolution of Sn-Pb will be postponed to a later publication. The oscillations during Sn-Pb stripping do not affect the analysis of the composition of the Sn-Pb. The stripping procedure has been used as a tool to determine the partial currents  $i_{Sn}$  and  $i_{Pb}$  for the deposition of Sn and Pb during the electroplating of the alloys.

### • Alloy compositions

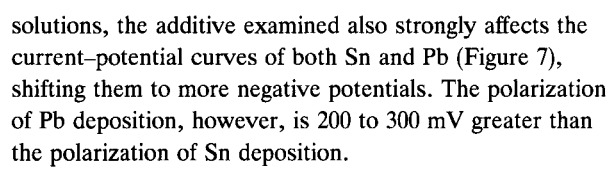
The IR-corrected polarization behavior of the partial currents  $i_{\rm Sn}$  and  $i_{\rm Pb}$  during deposition of the individual metals is shown on a logarithmic scale in Figure 7. At lower current densities, tin and lead have similar polarization curves in simple MSA solutions without additives. The slope  $\partial E/\partial \log i_M$  is very low for either metal M. The two metals are deposited at nearly the same potential.

Meibuhr et al. [27] have studied the kinetics of Sn deposition from stannous sulfate solutions. They have observed the extremely small activation polarization of deposition and have noted that Tafel linearity is not observed, a conclusion consistent with the curve in Figure 7 for Sn with no additive. Lead deposition in additive-free MSA solution has the same characteristic. In sulfate media [27], organic additives were found to have substantial effects on the electrode kinetics of Sn deposition. In MSA



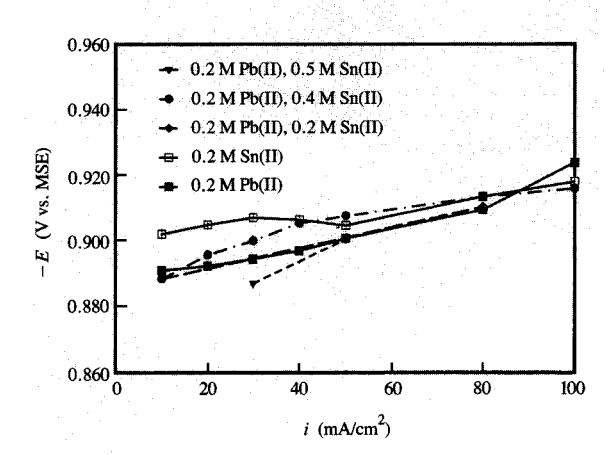


Potential dependence of the partial currents  $i_{\rm Sn}$  and  $i_{\rm Pb}$  from solutions containing 0.2  $M({\rm II})$  (M being Sn or Pb) in 1 N MSA, with and without 10 vol. % additive. All data have been corrected for IR drop.



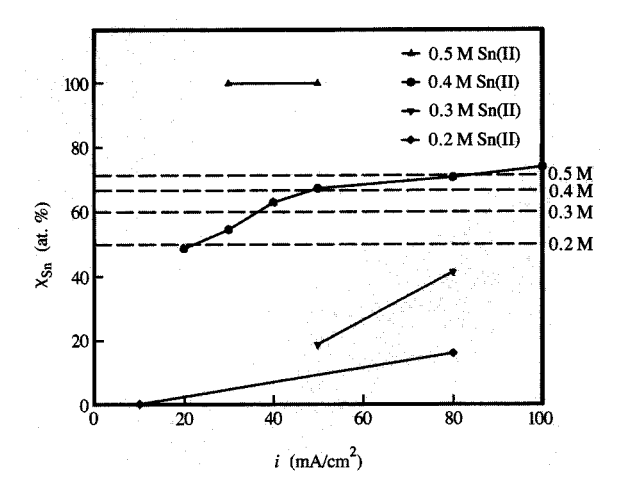
All of the metals and alloys examined were found to deposit with high current efficiencies (generally above ~95%) except for pure Sn from additive-free solutions; its current efficiency drops from 93% at 10 mA/cm² to 48% at 100 mA/cm². Tin under these conditions is a relatively good catalyst for H<sub>2</sub> evolution. On the other hand, Sn is deposited with nearly 100% current efficiency if the solution contains the additive.

Alloy deposition was examined in additive-free solutions having a constant Pb(II) concentration of 0.2 M and varying Sn(II) concentrations. The IR-corrected dependence of the potential on the total current density i is shown in Figure 8. In the absence of additive, the polarization curves for the alloys differed by only 50 to 100 mV, regardless of the Sn(II) concentration of the solution. Alloys were deposited under each of the conditions of Figure 8, but not all were suitable for the stripping analysis. Those with high Pb content passivated during electrodissolution under the conditions used, and a good end point was not obtained. For some of the films, a composition could be roughly estimated from the instantaneous ring current before the passivation occurred. This method was only used when the ring current was relatively constant, since a preferential dissolution of Sn would give a systematic overestimate of the Sn content.



#### Figure 8

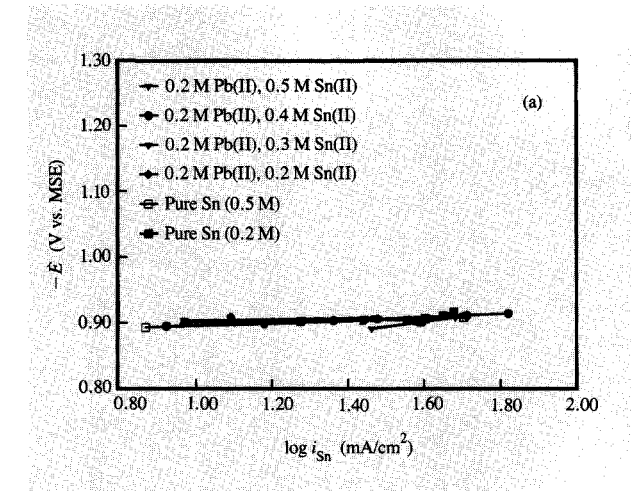
Potential dependence of the total plating current density i for various solution compositions.

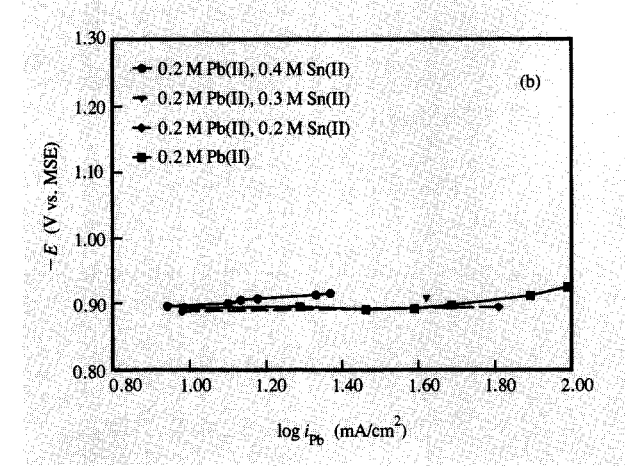


#### Figure 9

Composition of Sn-Pb alloy films deposited from additive-free solutions of 0.2 M Pb(II) in 1 N MSA containing various concentrations of Sn(II). Stripping was carried out at a disk current of 2 mA. The dashed lines designate the molar percentages of Sn(II) in solution.

The compositions of the deposits from additive-free solutions are summarized in **Figure 9**. The dashed lines designate the molar percentages of Sn(II) in solution. At Sn(II) levels of 0.3 M and below, the alloy is Pb-rich. At a Sn(II) concentration of 0.5 M, pure Sn is deposited. Only when the Sn(II) concentration is 0.4 M is an alloy





Potential dependence of the logarithm of the partial currents  $i_{\rm Sn}$  [in part (a)] and  $i_{\rm Pb}$  [in part (b)] for Sn-Pb alloy films deposited from additive-free solutions containing various amounts of Pb(II) and Sn(II) in 1 N MSA.

deposited that does not drastically differ in composition from the solution. The partial currents for Sn and Pb are shown in parts (a) and (b), respectively, of **Figure 10**. In additive-free MSA solutions, the polarization behavior for the Sn [Figure 10(a)] and the Pb [Figure 10(b)] is essentially the same for the alloy and for the pure metals.

For additive-containing solutions, the dependence of the potential on the total current density of plating is given in **Figure 11**. The presence of the additive changes the behavior of the system and the dependence on solution composition (compare Figures 8 and 11). With the additive, pure Pb is deposited at much more negative potentials than pure Sn. The alloys are deposited at intermediate potentials, and the behavior becomes more Sn-like as the Sn(II) concentration increases.

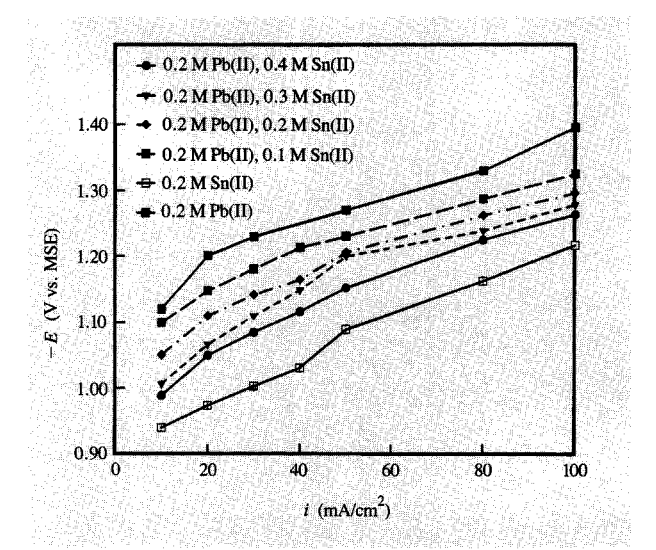
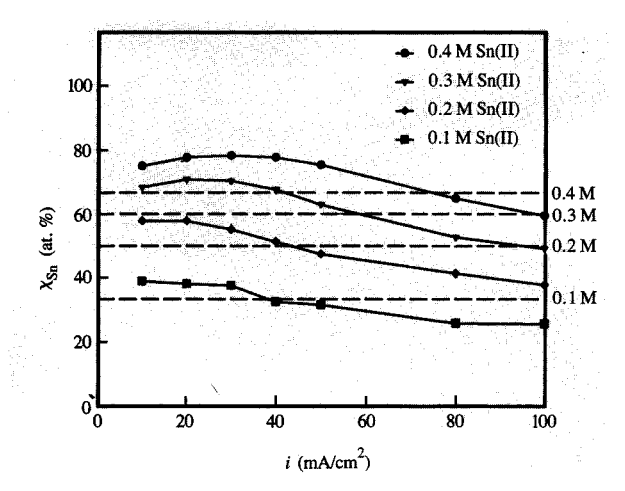


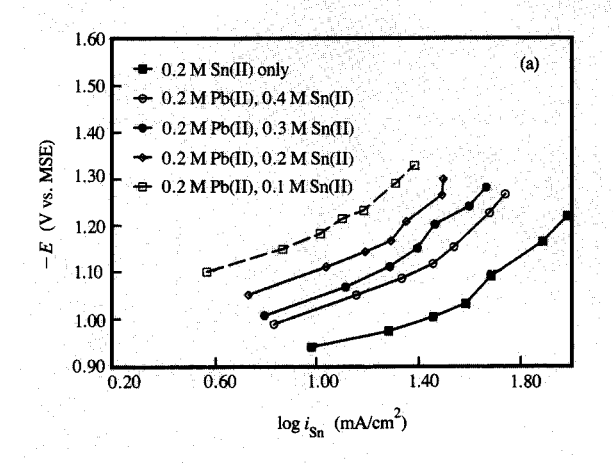
### Figure 11

Potential dependence of the total current density i for plating from solutions containing various amounts of Pb(II) and Sn(II) in 1 N MSA and 10 vol. % additive.

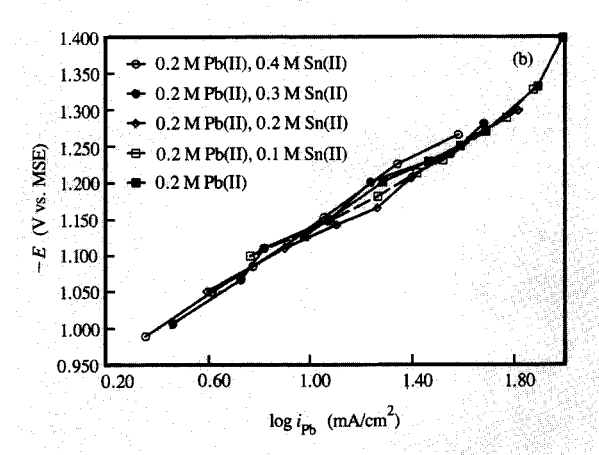
In the presence of the additive, the plated alloy films have approximately the same compositions as the solutions, as shown in Figure 12. The tin content decreases with increasing current density i, but the dependence of composition on current density is not strong. The partial currents for Sn and Pb deposition from additive-containing solutions, and their dependence on solution composition, are shown in parts (a) and (b) of Figure 13. The addition of 0.2 M Pb(II) substantially shifts the  $i_{Sn}$  curves [part (a)], but increasing the Sn(II) concentration causes the curves to move to less negative potentials. A direct comparison with the curve for pure Sn can only be made at a Sn(II) concentration of 0.2 M, however. Nonetheless, it is clear that the presence of Pb(II) affects the Sn deposition kinetics. The partial current  $i_{p_b}$  in the presence of the additive [part (b)], on the other hand, is similar in the presence and absence of Sn(II).

Several experiments were performed to assess the importance of the additive concentrations. The solutions used contained 0.2 M Pb(II), 0.4 M Sn(II), and various additive concentrations. A plating current density of 30 mA/cm² was used. **Table 2** shows the dependence of the alloy composition on the additive level in solution. There is an apparent minimum in the Sn level at an additive concentration of 0.5 vol. %. The data are too few to give a complete explanation; it is nonetheless clear that the composition of the deposit is insensitive to the concentration of the additive above about 1 vol. %.





Composition of Sn-Pb alloy films deposited from solutions containing 0.2 M Pb(II); 0.1, 0.2, 0.3, or 0.4 M Sn(II); 1 N MSA; and 10 vol. % of additive. Stripping analyses were carried out at a disk current of 2 mA. The dashed lines designate molar percentages of Sn(II) in solution.



### **Conclusions**

A rotating ring-disk stripping analysis using a HCl stripping medium can be used to determine the compositions of Sn-Pb alloys provided the Pb content of the alloys is not too high. The results of the analysis are insensitive to the stripping conditions despite a high sensitivity of the stripping behavior to the current density and rotation rate. When the metal flux away from the dissolving deposit is low and the Cl<sup>-</sup> concentration is high, large oscillations in the detected Sn(II)-oxidation current at the ring accompany very small oscillations in the potential of the dissolving disk. The oscillatory behavior is apparently caused by the preferential dissolution of Sn from the Sn-Pb alloy followed by the precipitation and redissolution of a sparingly soluble film of PbCl<sub>2</sub>. The exact mechanism of the oscillations needs further confirmation. It is possible, however, to ignore the oscillatory behavior for the purposes of alloy analysis. The partial currents  $i_{sn}$ and  $i_{ph}$  have been constructed from the analyses.

In the absence of the additive, the potential dependence of the partial currents for each metal is little affected by the presence of the other component of the alloy. The Sn-Pb deposit compositions, however, are very different from the solution compositions for most of the compositions examined. Even though both Pb(II) and Sn(II) are present at high concentrations in solution, relatively minor changes in the Sn(II) concentration greatly change the composition of the deposited alloy.

### Figure 13

Potential dependence of the logarithm of the partial currents  $i_{\rm Sn}$  [in part (a)] and  $i_{\rm Pb}$  [in part (b)] for deposition of Sn-Pb alloy films from solutions containing various amounts of Pb(II) and Sn(II) in 1 N MSA and 10 vol. % additive.

**Table 2** Dependence of Sn-Pb alloy film composition on additive concentration. The films were plated at 30 mA/cm<sup>2</sup> from solutions containing 0.2 M Pb(II) and 0.4 M Sn(II) in 1 N MSA.

Additive (vol. %)	χ <sub>sn</sub> (at. %)
0	55
0.5	55 39*
1	72
5	74
10	77

<sup>\*</sup>Ill-defined end point

The additive examined polarizes the deposition of both pure metals, Sn and Pb, but the Pb deposition curve is shifted by about 200 mV more than that of Sn. With the additive, there is control of the alloy composition over a wide composition range. The tin has a small effect on the polarization curve of Pb in the alloy, but the lead strongly polarizes Sn deposition relative to pure Sn. In the presence of the additive, the atomic Sn fraction of the film is not far from its molar fraction in solution.

The very fast kinetics of Sn and Pb deposition in additive-free solutions and the similarity of the deposition of the two metals make deposit composition extremely dependent on the deposition conditions. The additive, in polarizing the deposition reaction and slowing the reaction rates, permits controllable deposition of the alloy to be achieved over a wide composition range.

## Acknowledgments

The authors are grateful to M. Datta, H. Deligianni, G. Frankel, and L. T. Romankiw for their assistance in performing and understanding this work.

#### References

- 1. L. T. Romankiw, in Proc. Symp. Magnetic Materials, Processes, and Devices 90-8, L. T. Romankiw and D. A. Herman, Jr., Eds., The Electrochemical Society, Pennington, NJ, 1990, p. 39.
- 2. C. Rosenstein, Met. Finish. 88, 17 (1990).
- 3. J. Horkans, J. Electrochem. Soc. 126, 1861 (1979).
- 4. J. Horkans, Ibid. 128, 45 (1981).
- 5. P. C. Andricacos, C. Arana, J. Tabib, J. Dukovic, and L. T. Romankiw, Ibid. 136, 1336 (1989).
- S. Hessami and C. W. Tobias, *Ibid.* 136, 3611 (1989).
   H. Deligianni and L. T. Romankiw, in *Proc. Symp*. Magnetic Materials, Processes, and Devices 90-8, L. T. Romankiw and D. A. Herman, Jr., Eds., The Electrochemical Society, Pennington, NJ, 1990, p. 407.
- 8. H. Deligianni and L. T. Romankiw, Ibid., p. 423.
- 9. P. C. Andricacos, J. Tabib, and L. T. Romankiw, J. Electrochem. Soc. 135, 1172 (1988).
- 10. K. H. Wong and P. C. Andricacos, Ibid. 137, 1087 (1990).
- 11. J. Horkans, I. C. Hsu Chang, P. C. Andricacos, and E. J. Podlaha, Ibid. 138, 411 (1991)
- 12. D. Mandler and A. J. Bard, J. Electroanal. Chem. 307, 217 (1991).
- 13. A. J. Bard and L. R. Faulkner, Electrochemical Methods, John Wiley & Sons, Inc., New York, 1980, p. 302.
- 14. J. Wojtowicz, in Modern Aspects of Electrochemistry, Vol. 8, J. O'M. Bockris and B. E. Conway, Eds., Plenum Press, New York, 1972, p. 47.
- 15. H. P. Lee, K. Nobe, and A. Pearlstein, J. Electrochem. Soc. 132, 1031 (1985).
- 16. A. Pearlstein, H. P. Lee, and K. Nobe, Ibid. 132, 2159
- 17. L. T. Tsitsopoulos, T. T. Tsotsis, and I. A. Webster, Surf. Sci. 191, 225 (1987)
- 18. M. R. Bassett and J. L. Hudson, J. Electrochem. Soc. 137, 922 (1990).
- 19. M. R. Bassett and J. L. Hudson, Ibid. 137, 1815 (1990).
- 20. R. S. G. Doss and D. Deshmukh, J. Electroanal. Chem. 70, 141 (1976).
- 21. D. Sazou, M. Pagitas, and G. Kokkinidis, Electrochim. Acta 289, 217 (1990).

- 22. J. Stumper, R. Greef, and L. M. Peter, J. Electroanal. Chem. 310, 445 (1991).
- 23. D. H. Shen, W. Li, and K. Nobe, in Proc. Symp. on Critical Factors in Localized Corrosion 92-9, G. Frankel and R. C. Newman, Eds., The Electrochemical Society, Pennington, NJ, 1992.
- 24. S. G. Corcoran and K. Sieradzki, J. Electrochem. Soc. 139, 1568 (1992)
- 25. L. G. Sillen and A. E. Martell, Stability Constants of Metal-Ion Complexes, Special Publication 17, Chemical Society, London, 1964.
- 26. J. Kragten, Atlas of Metal-Ligand Equilibria in Aqueous Solution, Halsted Press, New York, 1978.
- 27. S. Meibuhr, E. Yeager, A. Kozawa, and F. Hovorka, J. Electrochem. Soc. 110, 190 (1963).

Received January 21, 1992; accepted for publication August 7, 1992

Jean Horkans IBM Research Division, Thomas J. Watson Research Center, P.O. Box 218, Yorktown Heights, New York 10598 (HORKANS at YKTVMV). Dr. Horkans is a Research Staff Member in the Manufacturing Research Department at the IBM Thomas J. Watson Research Center. She joined the Research Division in 1973 after completion of her Ph.D. in chemistry at Case Western Reserve University. Her interests are in electrochemical science and technology; she has investigated the electrodeposition and electroless deposition of metals and alloys, catalysis and the initiation of electroless deposition, thin film magnetic storage media, and conductive oxide electrodes. Dr. Horkans received awards in 1982 for studies of catalysts for electroless deposition and in 1991 for work on film disks. She is currently developing methods for analysis and control of plating solutions. She is a member of The Electrochemical Society.

I-Chia Hsu Chang IBM Research Division, Thomas J. Watson Research Center, P.O. Box 218, Yorktown Heights, New York 10598 (IHCHANG at YKTVMV). Mrs. Chang is an Associate Engineer in the Manufacturing Research Department at the IBM Thomas J. Watson Research Center. She received her B.S. in agricultural chemistry from the Chung-Hsing University of Taiwan, Republic of China, in 1963, and her M.S. in nutritional science from Colorado State University in 1967. Since joining IBM in 1989, she has worked on the deposition of thin film magnetic media for perpendicular recording, the analysis of electrodeposited alloys, and the monitoring and control of electroplating solutions. She is currently developing new analytical techniques for the monitoring and control of electroplating additives.

Panayotis C. Andricacos IBM Research Division, Thomas J. Watson Research Center, P.O. Box 218, Yorktown Heights, New York 10598 (PANOS at YKTVMV). Dr. Andricacos is Manager of Electrodeposition and Corrosion in the Manufacturing Research Department at the IBM Thomas J. Watson Research Center, and an Adjunct Associate Professor at Columbia University. He received his B.S., M.S., and D. Eng. Sc. degrees in chemical engineering from Columbia University in 1974, 1977, and 1980, respectively. In 1981 he joined the Lawrence Berkeley Laboratory, University of California, Berkeley, where he worked on oxygen reduction, transient behavior of rotating disk electrodes, and the application of UHV techniques to the study of plated atomic monolayers. Since joining IBM in 1984 as a Research Staff Member, Dr. Andricacos has worked on the applications of plating technology to the fabrication of magnetic devices, electronic packages, and semiconductor chips. He is a member of The Electrochemical Society and the International Society of Electrochemistry.